

Synthesis of Nanostructure Carbon Films Deposited by Microwave Plasma-Enhanced Chemical Vapor Deposition Technique at Room Temperature

Atul Bisht, Sreekumar Chockalingam, O. S. Panwar, A. K. Srivastava & Ajay Kumar Kesarwani

To cite this article: Atul Bisht, Sreekumar Chockalingam, O. S. Panwar, A. K. Srivastava & Ajay Kumar Kesarwani (2015) Synthesis of Nanostructure Carbon Films Deposited by Microwave Plasma-Enhanced Chemical Vapor Deposition Technique at Room Temperature, Fullerenes, Nanotubes and Carbon Nanostructures, 23:5, 455-462, DOI: [10.1080/1536383X.2014.921783](https://doi.org/10.1080/1536383X.2014.921783)

To link to this article: <http://dx.doi.org/10.1080/1536383X.2014.921783>



Accepted author version posted online: 07 Jul 2014.



Submit your article to this journal [↗](#)



Article views: 135



View related articles [↗](#)



View Crossmark data [↗](#)



Citing articles: 2 View citing articles [↗](#)

Synthesis of Nanostructure Carbon Films Deposited by Microwave Plasma-Enhanced Chemical Vapor Deposition Technique at Room Temperature

ATUL BISHT, SREEKUMAR CHOCKALINGAM, O. S. PANWAR, A. K. SRIVASTAVA,
and AJAY KUMAR KESARWANI

Polymorphic Carbon Thin Films Group, Physics of Energy Harvesting Division, CSIR-National Physical Laboratory, Dr. K. S. Krishnan Marg, New Delhi, India

Received 28 March 2014; accepted 3 May 2014

This paper reports the synthesis of nanostructure carbon (ns-carbon) films deposited by microwave plasma-enhanced chemical vapor deposition (MW PECVD) technique at low pressure and room temperature. ns-carbon films have been characterized by scanning electron microscopy, electron dispersive x-ray spectroscopic analysis, atomic force microscopy, Raman spectroscopy, X-ray diffraction, UV-visible spectroscopy and high-resolution transmission electron microscopy. The shape of nanostructure is changing from granular to sheet-like structure when the pressure increased from 55 to 110 mTorr.

Keywords: ns-carbon film, MW PECVD, SEM, XRD, HRTEM

Introduction

Recently, carbon nanostructures have received a great attention due to the wide variety of applications in electronics, mechanical, biomedical, and automotive industries (1–3). Formations of carbon nanostructures generally required high processing temperature. Carbon nanostructure such as spherical nanodiamond and nanosheets have been formed at high temperature necessary for the proper nucleation and transportation of building block in the plasma. A low processing temperature is required for the state of the art silicon-based semiconductor industries for the direct deposition of carbon-based nanostructures onto the silicon substrates. Therefore, lowering the processing temperature of carbon-based nanostructure is currently the focus of research worldwide. Recently, carbon nanosheets are of significant interest as they may contain many graphene layers (4, 5). Thomas and Rao (6) while synthesizing erected carbon sheets at very high temperature of about 800°C by electron cyclotron resonance plasma-enhanced chemical vapor deposition (ECR PECVD) found crumpled like semi-transparent sheets like structure on copper substrate. There are several plasma-based techniques

for the synthesis of carbon nanostructures such as radio frequency (RF) PECVD (7), Microwave (MW) PECVD (8), ECR PECVD (6), filtered cathodic vacuum arc (FCVA) technique (9) etc. Among these techniques, MW PECVD is a versatile technique for the deposition of carbon-based nanostructures such as ultra nanocrystalline diamond (10), carbon nanotube (CNT) (11, 12), carbon nanofiber (CNF) (13), and graphene (14, 15). MW PECVD has certain advantages over other techniques as it produces highly ionized plasma with high deposition rate, electrode less deposition, and capable of producing plasma from the low pressure to high pressure of several Torr. Recently, RF PECVD has been used for the growth of smooth diamond-like carbon (DLC) films at room temperature with improved surface roughness of SiAlON substrate from 4.13 to 0.47 nm (16). A low temperature deposition technique is preferred for the industrial applications particularly in electronic devices due to its easiness in depositing carbon films directly on low cost flexible substrates.

The present work reports the synthesis of carbon-based nanostructures by optimizing the process parameters used in MW PECVD technique at low pressure and room temperature. Carbon nanostructures are studied by variety of characterization techniques such as scanning electron microscopy (SEM), energy dispersive x-ray spectroscopic analysis (EDAX), atomic force microscopy (AFM), Raman spectroscopy, X-ray diffraction (XRD), UV-Visible spectroscopy, and high-resolution transmission electron microscopy (HRTEM). The formation of variety of carbon nanostructures have been explained on the basis of growth conditions.

Address correspondence to O. S. Panwar, Polymorphic Carbon Thin Films Group, Physics of Energy Harvesting Division, CSIR-National Physical Laboratory, Dr. K. S. Krishnan Marg, New Delhi 110012, India. E-mail: ospanwar@mail.nplindia.ernet.in

Color versions of one or more of the figures in this article can be found online at www.tandfonline.com/lfnn.

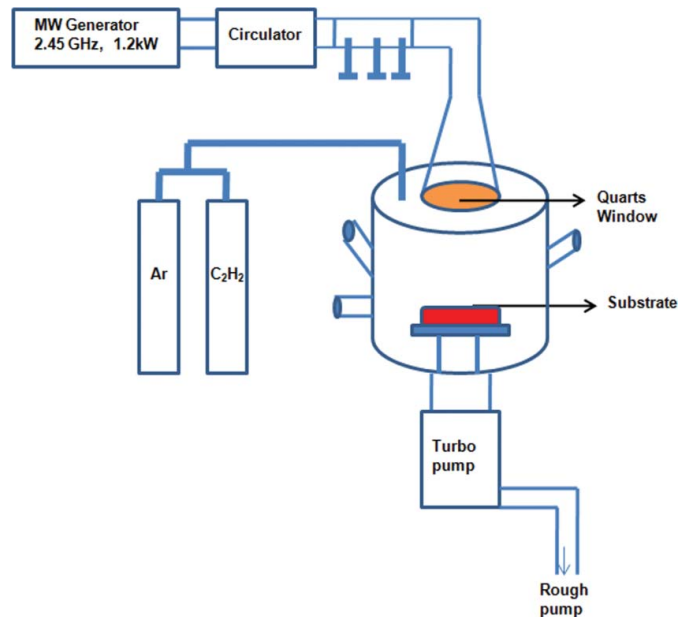


Fig. 1. Schematic of MW PECVD system.

Experimental Details

Details of Deposition System

ns-carbon films were deposited using 1.2 KW MW PECVD system at 2.45 GHz. The schematic diagram of MW PECVD system is shown in Figure 1. The microwave power from the generator was applied to the chamber by using circulator, three stub-tuners, waveguide, and a quartz window. Circulator protects the magnetron source from the reflected microwave power. Impedance matching of the wave guide and deposition chamber was achieved with the help of stub-tuner. The quartz plate acts as a divider between the deposition chamber and microwave generator and it acts as a transparent window for the microwave. To convert the transverse electric (TE) mode to the transverse magnetic (TM) mode, a rectangular to circular mode converter is used. The cavity in the TM mode delivers the microwave power more efficiently

than the TE mode to the gas to generate plasma. The ns-carbon films were deposited over well-cleaned silicon and quartz substrates at room temperature. A base pressure of $\sim 2 \times 10^{-6}$ Torr was achieved by the turbo molecular and rotary pump combination. The substrates were kept at ~ 12.5 cm below the quartz window. Prior to deposition, the substrates were also cleaned using argon plasma to remove the surface contaminations. These ns-carbon films were deposited at a fixed microwave power of 220 W. However, during deposition the working pressure was varied from 55 to 110 mTorr. This working pressure was achieved by feeding the acetylene (C_2H_2) and argon (Ar) gases to the chamber that changed the pressure from base pressure of $\sim 2 \times 10^{-6}$ Torr to working pressures of 55, 70, 80, and 110 mTorr. The details of deposition parameters used have been summarized in Table 1.

Details of Characterization

The ns-carbon films were characterized by morphological, structural and optical properties. The surface morphology of the sample was examined by scanning electron microscope (JEOL-JSM-7500 F SEM). The EDAX was carried out to detect the other elements present in the film. The Raman spectroscopy on these samples was performed using 514 nm excitation laser and notch filter at ~ 50 cm^{-1} at room temperature by a Renishaw spectrophotometer (micro-Raman model in Via Reflex). Measurement was performed at 5 mW incident power. X-ray diffraction was recorded from 10 to 60° with Bruker D8 Advanced x-ray diffractometer using CuK_{α} ($\lambda = 1.5418$ Å) radiation. The UV-Vis transmittance was recorded by a Perkin Elmer spectrophotometer (Lambda 950) in the range 200–800 nm. For HRTEM, samples were prepared by etching silicon substrates in HF + HNO_3 mixtures. On dilution of the mixtures with distilled water, the film floats on the surface of water. Subsequently, these self-supported films were lifted on a 200-mesh carbon-coated copper grid of 3.05 mm in diameter. HRTEM studies were carried out using a FEI Tecnai G2, F30-STWIN microscope with field emission gun source at the electron accelerating voltage of 300 KV to explore the nano- sub-nanoscale structural information present in the film.

Table 1. Deposition parameters and properties of different carbon nanostructures

S. No.	Parameters	Sample 1	Sample 2	Sample 3	Sample 4
1	Ar (SCCM)	80	85	90	95
2	C_2H_2 (SCCM)	20	15	10	5
3	Deposition pressure (mTorr)	55	70	80	110
4	D peak (cm^{-1})	1365.8	1347.2	1362.4	1368.6
5	G peak (cm^{-1})	1593.2	1601.2	1584.9	1593.3
6	2D peak (cm^{-1})	2700	2768	2699	2763
7	I_D/I_G	0.88	1.00	0.89	0.79
8	Size of ns-carbon (μm)	0.1 (width)	~ 0.2	~ 0.1	~ 0.1
9	Roughness (nm)	1.82	0.45	0.43	0.69
10	Transmittance (%) at 750 nm	90.4	93.0	93.6	94.5
11	E_g (eV)	4.1	3.8	3.7	3.3

Results and Discussion

SEM Study

Figure 2(a–d) shows the SEM micrographs of the films deposited at different pressures of (a) 55 mTorr, (b) 70 mTorr, (c) 80 mTorr, and (d) 110 mTorr. These micrographs clearly reveal the formation of various carbon nanostructures. The size and shape of nanostructures got changed when the pressure was varied from 55 to 110 mTorr. The ns-carbon film deposited at 55 mTorr showed the formation of multi-branched granular structures with a width of about $0.1\ \mu\text{m}$ (Figure 2a) in which different grains with varying structure were found to be interconnected. Some coagulated grain-like structure was also found at some place of the branched structure. The branched nanostructures have been found dispersed all over the film. Again nanostructured morphology was observed when the pressure was increased to 70 mTorr. Figure 2b shows small granular-like structure of dimension $\sim 0.2\ \mu\text{m}$. Spherical nanogranular structures were

also observed uniformly throughout the film. With the increase of C_2H_2 percentage, nanocrystallites have been found to be dispersed all over the film with varying density as shown in Figure 2(c). The inset shows the ns-carbon sphere of size $\sim 0.1\ \mu\text{m}$. Banerjee et al. (8) have found this type of dispersed spherical nanostructure at high temperature (200–300 °C) and high pressure (30–70 Torr). Amaral et al. (17) have found similar types of structures at very high temperature (650 °C) by hot wire CVD technique. It is interesting to note that the carbon nanostructures are formed at room temperature which otherwise generally requires high temperature processing. Temperature may be enhanced to some extent by the plasma of Ar and C_2H_2 which does not produce high temperature as hydrogen and C_2H_2 plasma produces. In Ar-rich plasma, C_2 radical is the main product due to the dissociation of $\text{C}\equiv\text{C}$ bond of C_2H_2 according to the reaction: $\text{Ar} + \text{C}_2\text{H}_2 \rightarrow \text{C}_2 + \text{H}_2$ energized by Ar molecule (18). C_2 radical plays a crucial role in the growth of such types of nanostructure. At low pressure up to few 10 Torr, electron's collision with the gas molecule is infrequent, thus the electron is having high

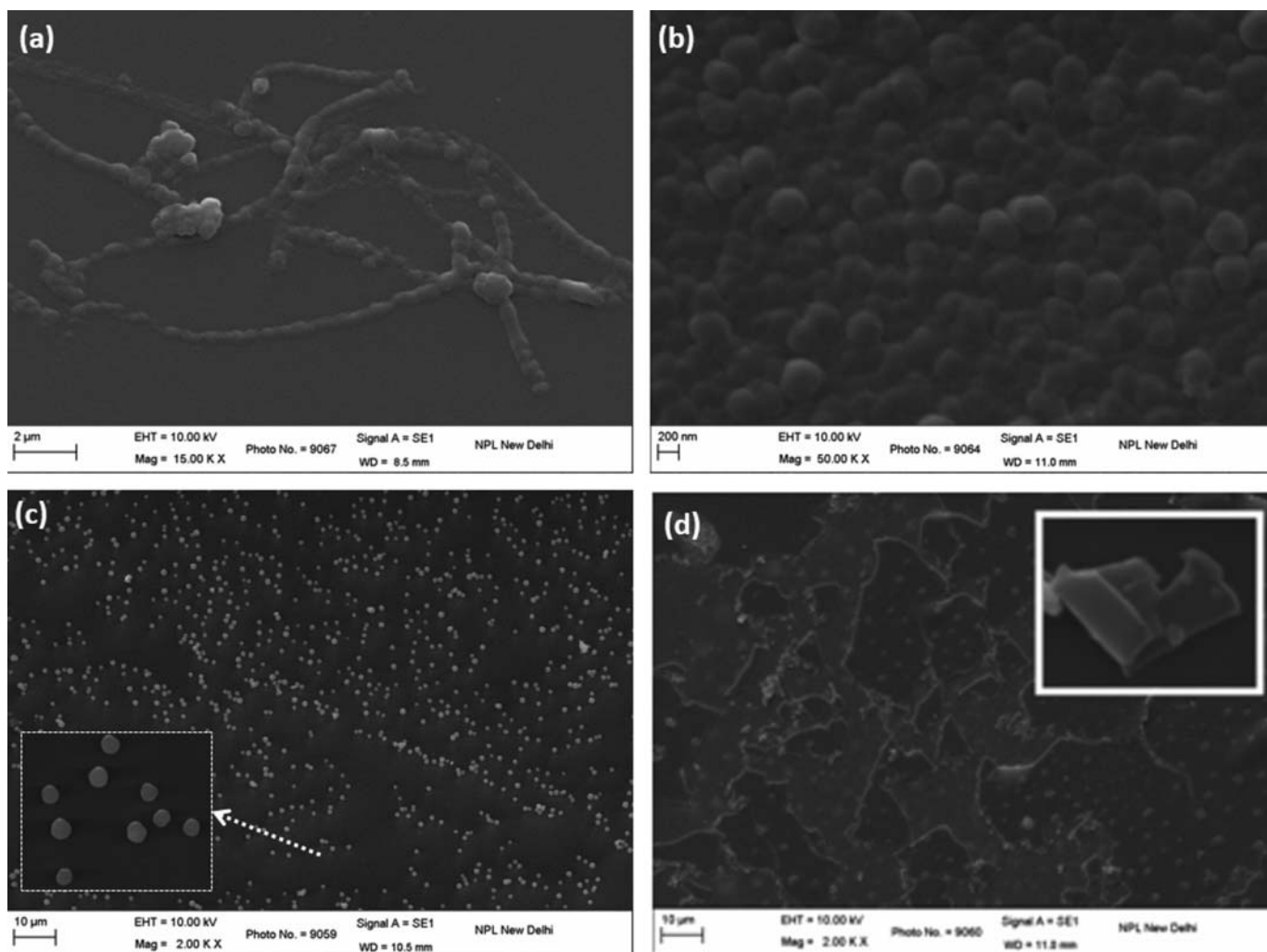


Fig. 2. SEM micrographs of ns-carbon films deposited at different pressures of (a) 55 mTorr, (b) 70 mTorr, (c) 80 mTorr, and (d) 110 mTorr, respectively.

energy in comparison to the energy at high pressure condition and the molecule dissociates generally by the electron collision (8). Increasing the Ar concentration may enhance the dissociation of C_2H_2 molecule which changed the structure from the branched granular to spherical carbon nanoparticles and sheet-like structure. Figure 2(d) shows the sheet-like structure incorporated with dispersed granular sphere of size $\sim 0.1 \mu\text{m}$ deposited at a pressure of 110 mTorr. Some spherical ns-carbon seems to be embedded in these sheets like structure. The size of ns-carbon formed at different pressures has been summarized in Table 1.

EDAX Study

EDAX measurement has been performed to detect the unwanted elements like oxygen contaminations present in the film in addition to carbon. Figure 3 shows the typical EDAX spectra of carbon sheets deposited at 70 mTorr pressure.

EDAX spectra revealed the presence of carbon, silicon (due to substrate) and negligible amount of oxygen which may be due to the surface contamination from the low purity of Ar gas used. Also EDAX uses such high energy X-rays (10 KeV) so that it may figure out oxygen from the bulk surface as the thickness of film is in nanometer range as silicon has also been detected.

AFM Study

Figure 4 shows the AFM micrographs of the ns-carbon films deposited at different pressures of (a) 55 mTorr, (b) 70 mTorr, (c) 80 mTorr, and (d) 110 mTorr. The morphology of ns-carbon observed in AFM images is in agreement with the SEM micrographs (Figure 2). The values of average surface roughness evaluated from the AFM micrographs have been summarized in Table 1. The values of surface roughness were found to be 1.82, 0.45, 0.43, and 0.69 nm, respectively, for

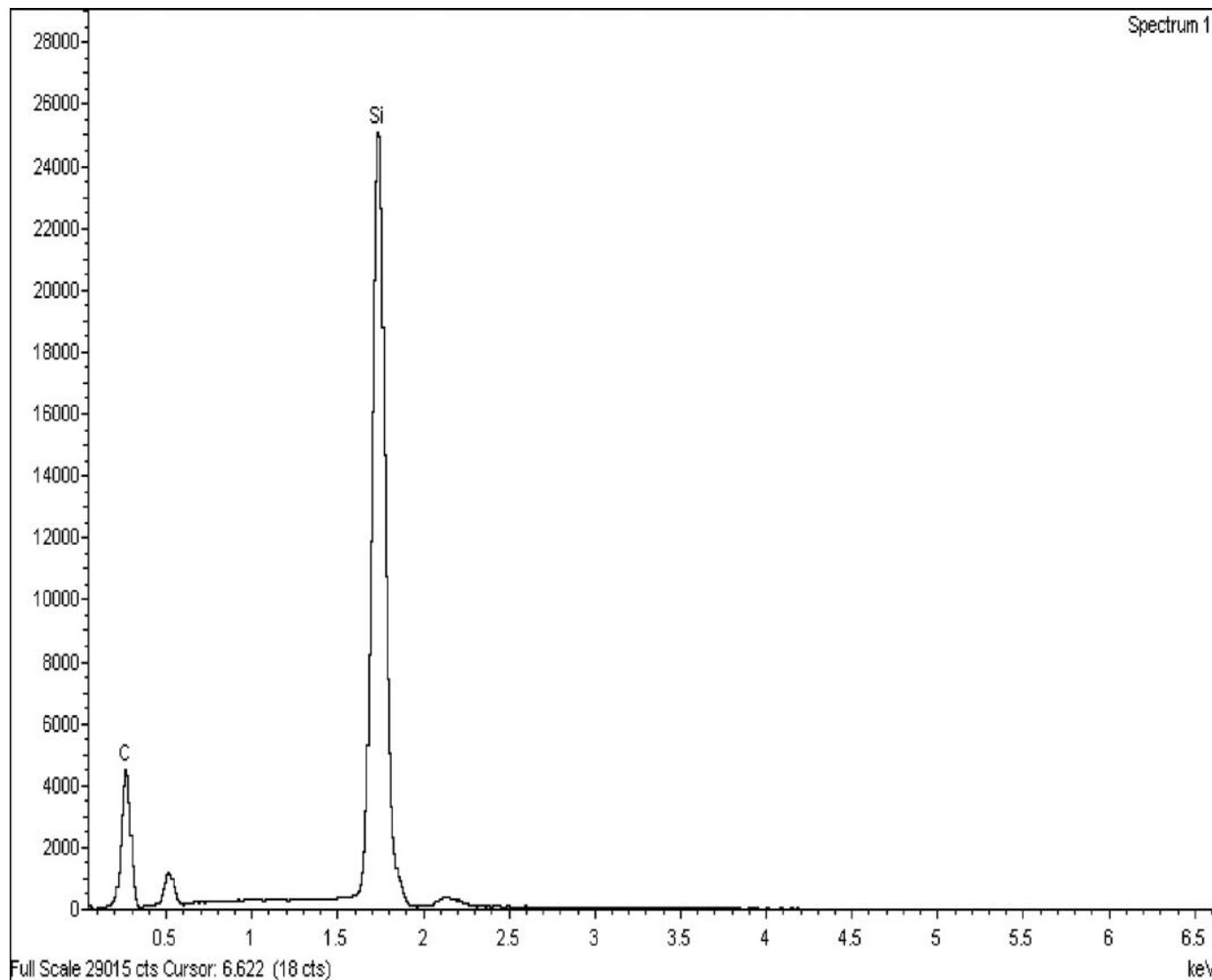


Fig. 3. Typical EDAX patterns of ns-carbon film deposited at 70 mTorr.

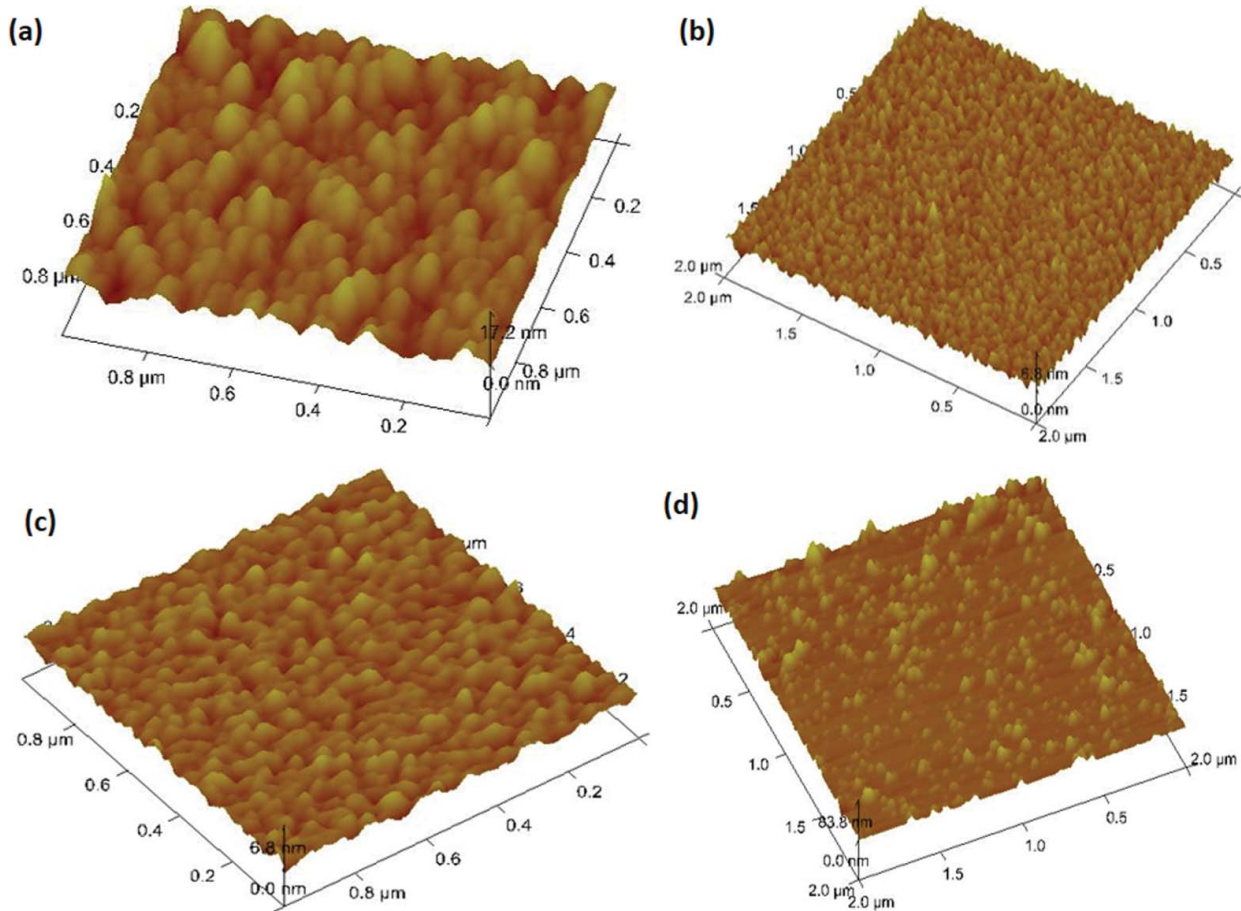


Fig. 4. AFM micrographs of ns-carbon films deposited at different pressures of (a) 55 mTorr, (b) 70 mTorr, (c) 80 mTorr, and (d) 110 mTorr, respectively.

the films deposited at different pressures of (a) 55 mTorr, (b) 70 mTorr, (c) 80 mTorr, and (d) 110 mTorr.

Raman Spectroscopy Study

Figure 5 shows the typical Raman spectra of ns-carbon films deposited at different pressures of (a) 55 mTorr, (b) 70 mTorr, (c) 80 mTorr, and (d) 110 mTorr. All the samples showed D peak around 1360 cm^{-1} to 1370 cm^{-1} , G peak around 1580 cm^{-1} to 1600 cm^{-1} , and very broad 2D peak around 2699 to 2768 cm^{-1} . Raman spectra which are an important tool for the characterization of carbon-based thin films reveal the well-known D and G peaks accompanied with very broad 2D peak in all the samples. G peak mainly arises due to E_{2g} symmetry of in-plane bond stretching motion of a pair of sp^2 bonded carbon atoms, whereas D peak around 1355 cm^{-1} is a breathing mode of A_{1g} and appeared due to the disorder in perfect graphite (19). 2D peak is due to the second order of the D peak which originates via a participation of two phonons with opposite wave vectors leading to momentum conservation (20). Accompanying the change in nanostructures in the films deposited at different pressures, there is no such dramatic change in the Raman spectra of these films. With the pressure variation, there is a change in the intensity and peak position of D and G peaks. The Raman spectra has been

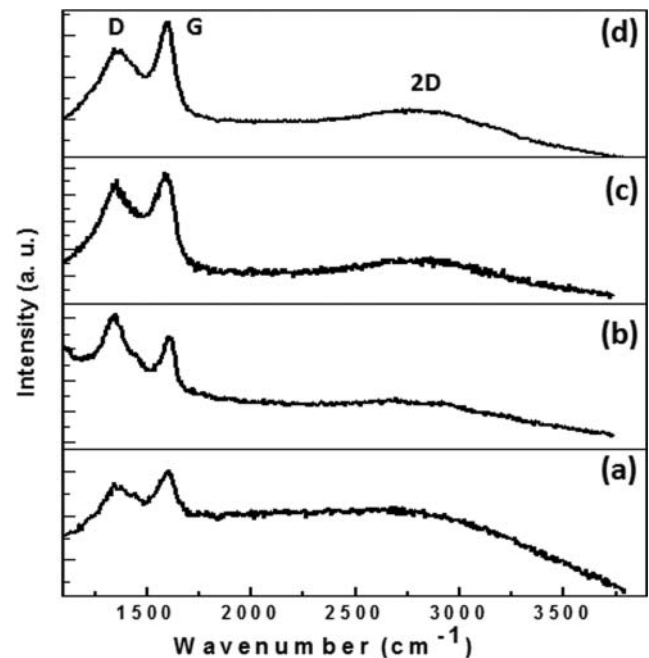


Fig. 5. Typical Raman spectra of ns-carbon films deposited at different pressures of (a) 55 mTorr, (b) 70 mTorr, (c) 80 mTorr, and (d) 110 mTorr, respectively.

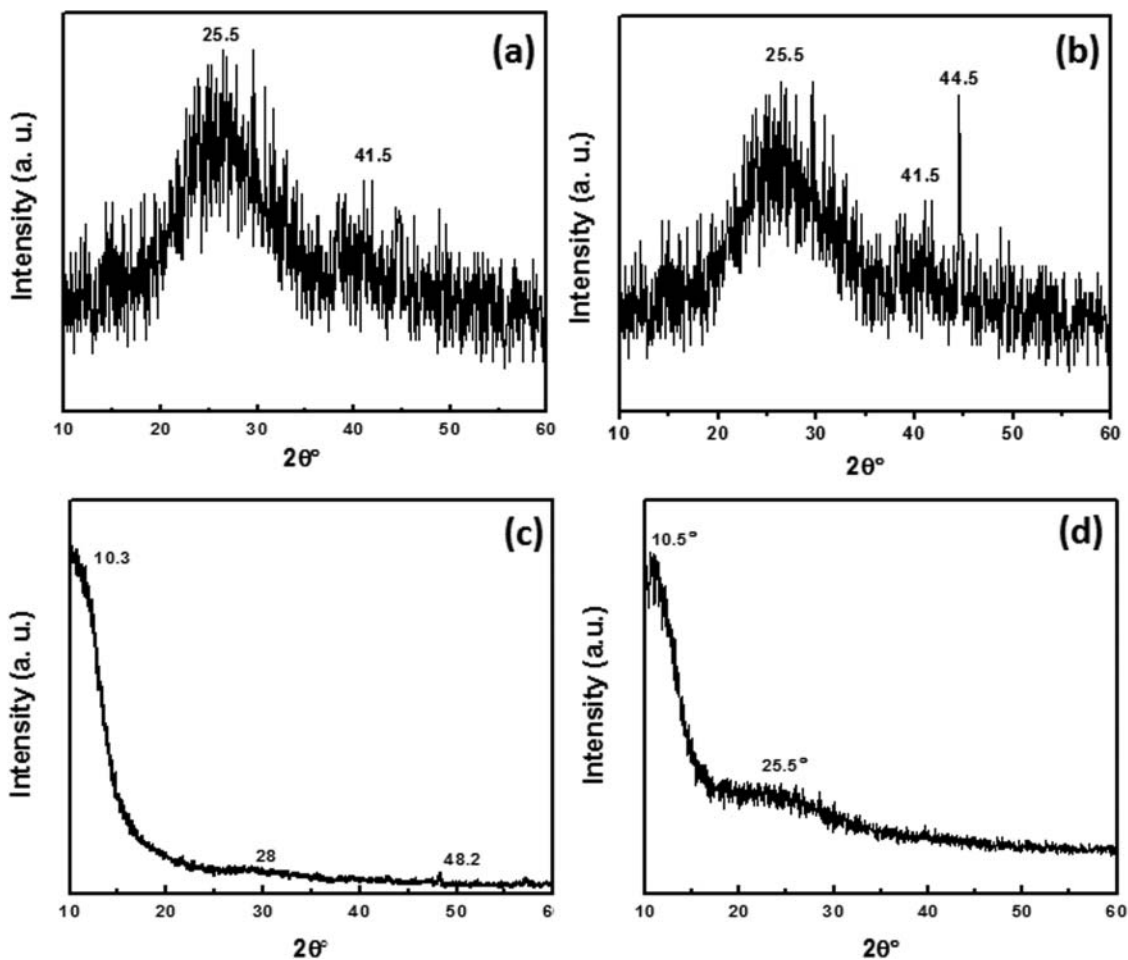


Fig. 6. Typical XRD patterns of ns-carbon films deposited at different pressures of (a) 55 mTorr, (b) 70 mTorr, (c) 80 mTorr, and (d) 110 mTorr, respectively.

deconvoluted into two Gaussian peaks to extract further information such as full width at half maximum (FWHM) and intensity of D and G peaks. The intensity ratio I_D/I_G and various peak positions of ns-carbon deposited at different pressures have been summarized in Table 1 along with the process parameters used in the growth of these films. In general, carbon-based thin films contain carbon atoms bonded as sp^2 and sp^3 hybridization. The Raman spectra particularly the peak position, intensity ratio of D and G peak, FWHM etc. depend upon the bonding arrangement of the film and hence the sp^2 - and sp^3 -bonded carbon atoms can be changed by these process parameters. Beeman et al. (21) suggested that the shift in G band toward the lower frequency is due to the increase of sp^3 -bonded atomic sites in amorphous carbon films. The I_D/I_G ratio and FWHM have been used as graphitization indication of the structure of carbon-based materials (22). It is evident from the table that I_D/I_G ratio is changing with the gas concentration. The I_D/I_G ratio is increasing from 0.88 to 1.00 up to 70 mTorr pressure and there is a reversal in the trend of I_D/I_G beyond this pressure.

XRD Pattern

The structural property was investigated by the XRD pattern. Figure 6 shows the typical XRD patterns of ns-carbon films deposited at different pressures of (a) 55 mTorr, (b) 70 mTorr, (c) 80 mTorr, and (d) 110 mTorr. All the samples showed a broad peak or hump at about 25.5° except in the sample 3 which showed a broad peak at about 28° . This is due to the amorphous phase present in all the films. Some other peaks at ~ 41.5 , 44.5 , and 48.2° also appear in Figure 6 (a, b, c). A peak at ~ 10.3 and $\sim 10.6^\circ$ appear in Figure 6c and Figure 6d, respectively. This peak is the characteristic of graphene oxide-based nanostructure. Srivastava et al. (23) also found similar XRD pattern who assigned the peak at 10.6° corresponding to $\langle 001 \rangle$ reflection of graphene oxide. Cai et al. (24) also found reflection corresponding to $\langle 001 \rangle$ plane of graphene oxide at $2\theta = 10.9^\circ$. The XRD pattern revealed the mixture of amorphous and nanocrystalline phase due to the presence of broad peak or hump at $\sim 25.5^\circ$ and some sharp peaks. The peaks at 41.5 , 44.5 , and 48.2° may be attributed to the diamond reflection (25).

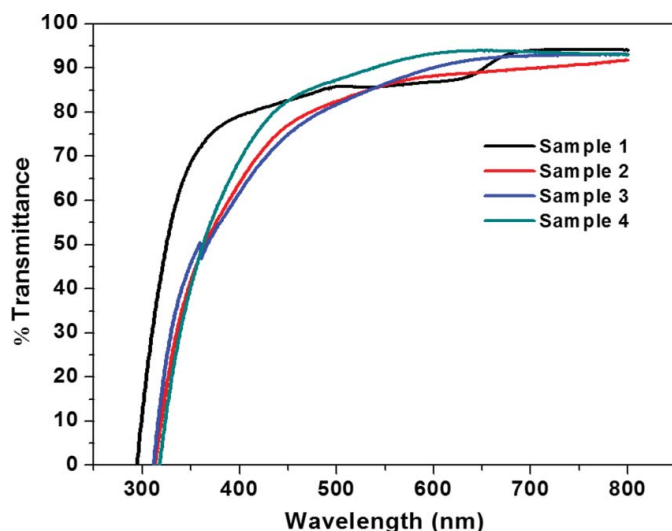


Fig. 7. Typical transmittance curves of ns-carbon films deposited at different pressures of (a) 55 mTorr, (b) 70 mTorr, (c) 80 mTorr, and (d) 110 mTorr, respectively.

UV-Visible Spectroscopy Study

Figure 7 shows the transmittance spectra of ns-carbon films deposited at different pressures. The values of transmittance at 750 nm of all the samples have been summarized in Table 1. It is evident from the curves that all the films exhibit the high value of transmittance (>90%) in near IR region. ns-carbon film deposited at 110 mTorr showed the highest value of transmittance of 94.5% among all the samples studied. The value of the transmittance increased from 90.4 to 94.5% with the increase of gas pressure used in the deposition of these ns-carbon films. The C_2H_2 concentration and hence the amount of carbon increased with the decrease of total pressure. This may be the reason for the reduction in the value of transmittance. Optical band gap (E_g) has been measured by Tauc's plot generally used for amorphous materials (26). Under the assumption of parabolic band in amorphous solids, the relation between the absorption coefficient (α) and energy ($h\nu$) is given by $(\alpha h\nu)^{1/2} = B(h\nu - E_g)$ where B is a constant. The value of E_g is evaluated from the intercept obtained by extrapolating the linear part of the $(\alpha h\nu)^{1/2}$ versus $h\nu$ curve to zero abscissa. The values of E_g of all the samples deposited at different pressures are evaluated to be 4.1, 3.8, 3.7, and 3.3 eV which are summarized in Table 1.

HRTEM Study

HRTEM was employed to characterize the ns-carbon film deposited at 110 mTorr pressures. In general, the microstructure was constituted of graphene nanosheets (Figure 8a) with almost transparent appearance. Most of the region of thin films was uniformly consisted of such structure. An atomic scale image with an adequate tilting revealed a honeycomb structure of these nanosheets with hexagonal fringes with an interseparation of about 0.34 nm (inset in Figure 8a). These

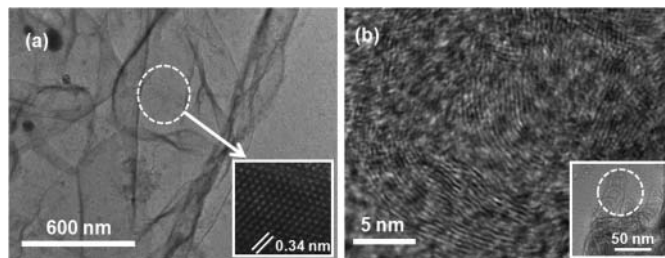


Figure 8. Typical HRTEM micrographs showing (a) nanosheets of graphene, and (b) atomic scale images of carbon nanotubes of ns-carbon film deposited at 110 mTorr: Insets: (a) honeycomb structure of graphene, and (b) overlapped region of several carbon nanotubes.

fringes are the characteristic of graphene polymorph of carbon. The region, magnified at atomic scale, is encircled with white dotted line in Figure 8a. It was further possible to explore in thin films that at instances there are few bunches of ultrathin circular rings piled up over each other (inset in Figure 8b). A selective region (white-dotted encircled region in the inset of Figure 8b) was magnified to atomic scale to investigate the actual morphology of these inter-abutting rings. It was interesting to note that these rings are short length carbon nanotubes with distinct multi-walled structure. Some of these nanotubes inter-mingled to each other in the microstructure are displayed as in Figure 8b.

Conclusions

Different types of carbon nanostructures have been grown by using MW PECVD technique at room temperature by varying the deposition pressure from 55 to 110 mTorr. It has been found that the deposition pressure plays a significant role in controlling the nanostructure of carbon films. Surface roughness of the film decreased from 1.82 to 0.43 nm with the increase of pressure up to 80 mTorr and beyond 80 mTorr the value of surface roughness increases to 0.69 nm. The values of transmittance increased from 90.4 to 94.5% and those of E_g decreased from 4.1 to 3.3 eV with the increase of pressure from 55 to 110 mTorr. The HRTEM along with the SEM micrographs reveal sheet-like structure of the carbon samples deposited at 110 mTorr dispersed in the amorphous matrix.

Acknowledgments

The authors are grateful to Prof. R. C. Budhani, Director, CSIR-National Physical Laboratory, New Delhi, India, for his kind permission to publish this paper. They wish to thank Mr. K. N. Sood for providing the SEM micrographs and EDAX data, to Mr. Sandeep Singh for providing AFM micrographs and to Dr. N. Vijayana for providing X-ray diffraction patterns and to Mr. Jagdish Chand for providing technical help.

Funding

Mr. Atul Bisht and Mr. Ajay Kumar Kesarwani are grateful to the University Grant Commission (UGC) and Council of Scientific Industrial Research (CSIR), Government of India, respectively, for the financial assistance during the course of this work.

References

- Robertson, J. (2014) Diamond-like carbon films, properties and applications. *Comprehensive Hard Mater.*, 3: 101–139.
- Kumar, S., Dwivedi, N., Rauthan, C. M. S., and Panwar, O. S. (2010) Properties of nitrogen diluted hydrogenated amorphous carbon (n-type a-C: H) films and their realization in n-type a-C: H / p-type crystalline silicon heterojunction diodes. *Vacuum*, 84 (7): 882–889.
- Hauert, A. (2003) Review of modified DLC coatings for biological applications. *Diam. Relat. Mater.*, 12 (3–7): 583–589.
- Tiwari, J. N., Tiwari, R. N., Singh, G., and Lin, K. L. (2011) Direct synthesis of vertically interconnected 3-D graphitic nanosheets on hemispherical carbon particles by microwave plasma CVD. *Plasmonics*, 6: 67–73.
- Bo, Z., Yang, Y., Chen, J., Yu, K., Yan, J., and Cen, K. (2013) Plasma-enhanced chemical vapor deposition synthesis of vertically oriented graphene nanosheets. *Nanoscale*, 5: 5180–5204.
- Thomas, R., and Rao G. M. (2012) Synthesis of free standing carbon nanosheet using electron cyclotron resonance plasma enhanced chemical vapor deposition. *Appl. Surf. Sci.*, 258: 4877–4880.
- Vizireanu, S., Mitu, B., Luculescu, C. R., Nistor, L. C., and Dinescu, G. (2012) PECVD synthesis of 2D nanostructured carbon material. *Surf. Coat. Technol.*, 211: 2–8.
- Banerjee, A., and Das, D. (2013) Realizing a variety of carbon nanostructures at low temperature using MW-PECVD of (CH₄ + H₂) plasma. *Appl. Surf. Sci.*, 273: 806–815.
- Panwar, O. S., Kesarwani, A. K., Dhakate, S. R., Singh, B. P., Rakshit, R. K., Bisht, A., and Chockalingam, S. (2013) Few layer graphene synthesized by filtered cathodic vacuum arc technique. *J. Vac. Sci. Technol. B*, 31 (4): 040602 (5)
- Cheng, H. F., Horng, C. C., Chiang, H. Y., Chen, H. C., and Lin, I. N. (2011) Modification on the microstructure of ultra nanocrystalline diamond films for enhancing their electron field emission properties via a two-step microwave plasma enhanced chemical vapor deposition process. *J. Phys. Chem. C*, 115 (28): 13894–13900.
- Meyyappan, M., Delzeit, L., Cassell, A., and Hash, D., (2003) Carbon nanotube growth by PECVD: A review. *Plasma Sources Sci. Technol.*, 12: 205–216.
- Hoshino, Y., Arima, H., Saito, Y., and Nakata, J. (2012) Growth of single-walled carbon nanotubes from hot-implantation-formed catalytic Fe nanoparticles assisted by microwave plasma. *Appl. Surf. Sci.*, 258: 2982–2988.
- Boskovic, B. O., Vlad, S., Zeze, D. A., Forrest, R. D., Silva, S. R. P., and Haq, S. (2004) Branched carbon nonofiber network synthesis at room temperature using radio frequency supported microwave plasma. *J. Appl. Phys.*, 96 (6): 3443–3446.
- Jiang, L., Yang, T., Liu, F., Dong, J., Yao, Z., Shen, C., Deng, S., Xu, N., Liu, Y., and Gao, H. J. (2013) Controlled synthesis of large-scale, uniform, vertically standing graphene for high-performance field emitters. *Adv. Mater.*, 25: 250–255.
- Kim, Y., Song, W., Lee, S. Y., Jeon, C., Jung, W., Kim, M., and Park, C. Y. (2011) Low temperature synthesis of graphene on nickel foil by microwave plasma chemical vapor deposition. *Appl. Phys. Lett.*, 98: 263106 (3).
- Bisht, A., Chockalingam, S., Tripathi, R. K., Dwivedi, N., Dayal, S., Kumar, S., Panwar, O. S., Chand, J., Singh, S., and Kesarwani, A. (2013) Improved surface properties of β -SiAlON by diamond-like carbon coatings. *Diam. Relat. Mater.*, 36: 44–50.
- Amaral, M., Oliveira, F. J., Belmonte, M., Fernandes, A. J. S., Costa, F. M., and Silva, R. F. (2004) Hot-filament chemical vapor deposition of nanodiamond on silicon nitride substrates. *Diam. Relat. Mater.*, 13: 643–647.
- Teii, K., Shimada, S., Nakashima, M., and Chuang, A. T. H. (2009) Synthesis and electrical characterization of n-type carbon nanowall. *J. Appl. Phys.*, 106: 084303 (6).
- Ferrari, A. C. and Robertson, J. (2000) Interpretation of Raman spectra of disordered and amorphous carbon. *Phys. Rev. B*, 20: 14095–14107.
- Reina, A., Jia X., Ho, J., Nezich, D., Son, H., Blovic, V., Dresselhouse, M. S., and Kong, J. (2009) Large area, few-layer graphene films on arbitrary substrates by chemical vapor deposition. *Nano Lett.*, 9, 30–35.
- Beeman, D., Silverman, J., Lynds, R., and Anderson, M. R., (1984) Modeling studies of amorphous carbon. *Phys. Rev., B*, 30: 870–875.
- Santra, T. S., Bhattacharyya, T. K., Tseng, F. G., and Barik, T. K. (2012) Influence of flow rate on different properties of diamond-like nanocomposite thin films grown by PECVD. *AIP Adv.*, 2: 022132 (10).
- Srivastava, S., Jain, K., Singh, V. N., Singh, S., Vijayan, N., Dilawar, N., Gupta, G., and Senguuttuvan, T. D. (2012) Faster response of NO₂ sensing in graphene-WO₃ nanocomposites. *Nanotechnology*, 23: 205501 (7).
- Cai, D. and Song, M. (2007) Preparation of fully exfoliated graphite oxide nanoplatelets in organic solvents. *J. Mater. Chem.*, 17: 3678–3680.
- Standard data, *JCPDS Card numbers*, 898493, 791471 and 898494.
- Tauc, J., Grigorovici, R., and Vancu, A. (1966) Optical properties and electronic structure of amorphous germanium. *Phys. Status Solidi (b)*, 15: 627–637.